Multiple Photonic Responses in Films of Organic-Based Magnetic Semiconductor V(TCNE)$_x$, $x \sim 2$

Jung-Woo Yoo,[1] R. Shima Edelstein,[1] D. M. Lincoln,[2] N. P. Raju,[1] C. Xia,[2] K. I. Pokhodnya,[1,3]
Joel S. Miller,[3] and A. J. Epstein[1,2]

[1]*Department of Physics, The Ohio State University, Columbus, Ohio 43210-1117, USA*
[2]*Department of Chemistry, The Ohio State University, Columbus, Ohio 43210-1173, USA*
[3]*Department of Chemistry, University of Utah, Salt Lake City, Utah 84112-0850, USA*
(Received 6 August 2006; published 14 December 2006)

Concomitant photoinduced magnetic and electrical phenomena are reported for the organic-based magnetic semiconductor V(TCNE)$_x$ ($x \sim 2$; TCNE = tetracyanoethylene; magnetic ordering temperature $T_c \sim 400$ K). Upon optical excitation (457.9 nm), the system can be trapped in a thermally reversible photoexcited state, which exhibits reduced magnetic susceptibility and increased conductivity with a simultaneous change in IR absorption spectrum. The multiple photonic effects in V(TCNE)$_x$ are proposed to originate from structural changes induced by internal excitation in (TCNE)$^-$ anions, which lead to relaxation to a long-lived metastable state.

Materials possessing novel combinations of magnetic and electrical properties, such as multiferroic oxides, and dilute magnetic semiconductors (DMS), have received great attention in recent years, especially in the area of spintronics, which exploits both the spin and electrical properties of charge carriers in a material [1–3]. Organic-based magnets provide an alternative pathway in achieving novel characteristics of materials with a tunability of magnetic and electronic properties via organic methodologies. V(TCNE)$_x$, ($x \sim 2$), is a particularly interesting system because it features a magnetic ordering temperature above room temperature ($T_c \sim 400$ K) with a fully spin-polarized conduction band [4–7]. Meanwhile, the control of magnetic properties by light has also been an active area of research that has attracted considerable attention in recent years. Extensive studies have been performed on a variety of systems that display magnetic bistability and/or photo-induced magnetism (PIM). These include cyanometalate-based magnets [8–10], spin crossover complexes [11,12], dilute magnetic semiconductors [13], doped manganites [14], and organic-based magnet [Mn(TCNE)$_x \cdot$ y(CH$_2$Cl$_2$)] [15]. Challenges towards multiple functionality in a single system include design and preparation of materials that exhibit both long-range magnetic order and photoinduced magnetization as well as light-tunable transport properties.

We report here unusual multiple photonic phenomena in CVD-deposited films of the organic-based magnetic semiconductor V(TCNE)$_x$. Photoinduced magnetism and conductivity are observed and correlate with each other and suggest reversible trapping of a photoexcited metastable state induced by structural change, as indicated in photo-induced IR absorption spectra.

The organic-based magnet V(TCNE)$_x$ is a member of the M(TCNE)$_x$ family (M = V, Fe, Mn, Co, Ni) [16] of magnets. The magnetic ordering in this class of magnet is based on direct exchange between the unpaired electrons in (TCNE)$^-$ π^* orbitals, whose spin ($S = 1/2$) is distributed over the entire anion [17], and the spin in the transition metal ions. The V(TCNE)$_x$ is a ferrimagnet of uncompensated antiparallel (TCNE)$^-$ ($S = 1/2$) and V^{2+} ($S = 3/2$) spins with a $T_c \sim 400$ K [4]. Extended x-ray absorption fine structure (EXAFS) studies indicate that V^{2+} has octahedral coordination with N [18]. The conductivity is semiconductorlike and varies with preparation in the range 10^{-2}–10^{-4} S cm^{-1} with an activation energy of ~ 0.5 eV at room temperature [7]. The π^* band in (TCNE)$^-$ is split by the on-site Coulomb repulsion [6,7,19,20] into two subbands with opposite spin polarization [6,7], one occupied and one unoccupied. The anomalous positive magnetoresistance in V(TCNE)$_x$ reflects the spin-polarized nature of the energy bands and the role of magnetic energy in the band gap [6,7].

The CVD-deposited solvent-free films of V(TCNE)$_x$ were prepared under Ar flow in a controlled atmosphere (O$_2 < 0.1$ ppm, H$_2$O < 1.0 ppm) [5]. Typical thickness of films used is ~ 500 nm. The morphology of CVD-deposited V(TCNE)$_x$ film shows homogeneous surface and lack of polycrystalline granular features [21]. The samples for magnetic measurements were deposited on thin glass substrates. Two-terminal gold electrodes with a width 2 mm and a thickness of 200 nm separated by a gap of 100 μm were used for transport measurement, as the contact resistance is negligible in comparison of 2-probe and 4-probe measurements [22]. Samples for optical absorption were deposited on quartz (for UV-Vis-NIR) and KBr (for IR). All measurements were performed in air-protective sample holders, as the sample is sensitive to oxygen.

The dc magnetization was recorded on a Quantum Design MPMS-5 magnetometer. The dc conductivity was measured in a Quantum Design PPMS-9 platform with an

additional sample probe attached with fiber optic illumination system and Keithley 617 electrometer. UV-Vis-NIR optical absorption was measured with a Perkin-Elmer Lambda-19 spectrometer. Infrared spectra were recorded on a Bruker IFS 66v/s FTIR spectrometer. An Ar-ion laser was used for illumination. All instruments were equipped with a fiber-optics illumination system.

The effect of illumination on the field-cooled magnetization (M_{fc}), measured at 10 K, in a static magnetic field of 50 Oe is shown in Fig. 1(a). Upon excitation with the $\lambda \sim 457.9$ nm argon laser line (light intensity $I \sim 20$ mW/cm^2), which corresponds to the $\pi \to \pi^* + U_c$ [$U_c =$ Coulomb repulsion energy for two electrons in the (TCNE) π^* orbital], the magnetization decreases and reaches saturation in about 6 h. After turning the laser off, M_{fc} exhibits an additional decrease in Fig. 1(a), attributed to cooling of the sample with a estimated $\Delta T < 5$ K (M_{fc} increases with the increase of T at 10 K [Fig. 1(b)]). The photoexcited state is preserved even in the dark after illumination. For example, the photoinduced magnetization decreases by only ~0.5% after one week at 10 K, which gives a lifetime $>10^7$ s by assuming exponential
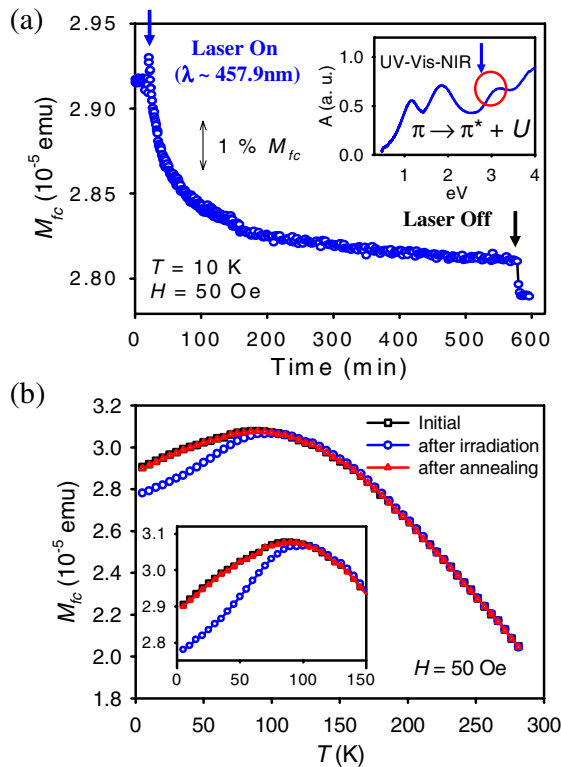
FIG. 1 (color online).   (a) Effects of argon laser excitation ($\lambda \sim$ 457.9 nm, light intensity $I \sim 20$ mW/cm^2, at 10 K) on the field-cooled magnetization of V(TCNE)$_x$ film. UV-Vis-NIR spectra of absorption shown in inset indicating $\pi \to \pi^* + U_c$ excitation around 3 eV. (b) Temperature dependence of field-cooled magnetization [black: before illumination, blue: after illumination ($\lambda \sim 457.9$ nm, $I \sim 20$ mW/cm^2, at 10 K for 10 h), red: after annealing sample (to 280 K and waiting for 10 min)].

relaxation of PIM. The UV-Vis-NIR absorption of inset in Fig. 1(a) shows the $\pi \to \pi^* + U_c$ excitation band, in the region of 2.5–3.5 eV, the same excitation band which initiates photoinduced magnetism in Mn(TCNE)$_x$ [15].

The temperature dependence of magnetization, for both ground and photoexcited states, is displayed in Fig. 1(b). The field-cooled magnetization (M_{fc}) increases monotonically as the temperature is lowered from room temperature to 90 K, where it has a maximum, and decreases upon lowering temperature further to 5 K, which suggests a reentrant transition at $T_r \sim 90$ K. After illumination ($\lambda \sim 457.9$ nm, $I \sim 20$ mW/cm^2, 10 K for 10 h), there is a substantial decrease in M_{fc} below 90 K, and T_r is slightly shifted to higher temperature ($T_r \sim 100$ K in photoexcited state) as shown in inset of Fig. 1(b). While the photoinduced effects are present below the reentrance temperature, no PIM is detected above the reentrance temperature. The stability of the photoexcited state was studied by warming above 150 K and waiting for 10 min then cooling it back to 5 K, and repeating the measurement of M_{fc}. Annealing the irradiated sample to 150 K does not erase the PIM as 90% of PIM is still maintained. The photoexcited state can be fully recovered to the ground state by warming the sample to 250 K or above. The red curve in Fig. 1(b) shows complete recovery of the ground state without any degradation of the sample. It is noticed that although there is substantial decrease of magnetization at low field, no change in saturation magnetization was found over the entire temperature region (5–300 K). Therefore, there is no photoinduced change in the number of unpaired spins and the mechanism of PIM is different from that of charge transfer induced PIM in cyanometalate-based magnets [8–10].

The light-induced effects on the conductivity of the CVD-deposited V(TCNE)$_x$ film are displayed in Fig. 2. In Fig. 2(a), the material was illuminated at 120 K by an Ar-ion laser ($\lambda \sim 457.9$ nm, $I \sim 20$ mW/cm^2). After 2 h of illumination, the resistivity of V(TCNE)$_x$ film decreases by a factor of 3. The shift of resistivity after turning off the laser is due to the thermal heating effect during the light irradiation with a $\Delta T < 2$ K. The photoinduced conductivity can be erased by warming the sample above 250 K, similar to the effect of heating on PIM. The inset in Fig. 2(a) shows Ohmic i-V curves for both ground and photoexcited states at 120 K. After 2 h of illumination, the i-V slope is increased by a factor of 3.

Detailed conductivity studies for both solution-prepared powders and CVD-deposited films of V(TCNE)$_x$ revealed that the electronic transport for these samples has semiconductorlike behavior with a activation gap ~0.5 eV [6,7,23]. Normalized resistances as a function of temperature for both ground and photoexcited states are shown in Fig. 2(b). After illumination, the temperature dependence of resistivity substantially deviates from the ground state at low temperature. However, $\rho(T)$ for both ground and photoexcited states are nearly indistinguishable as the tem-
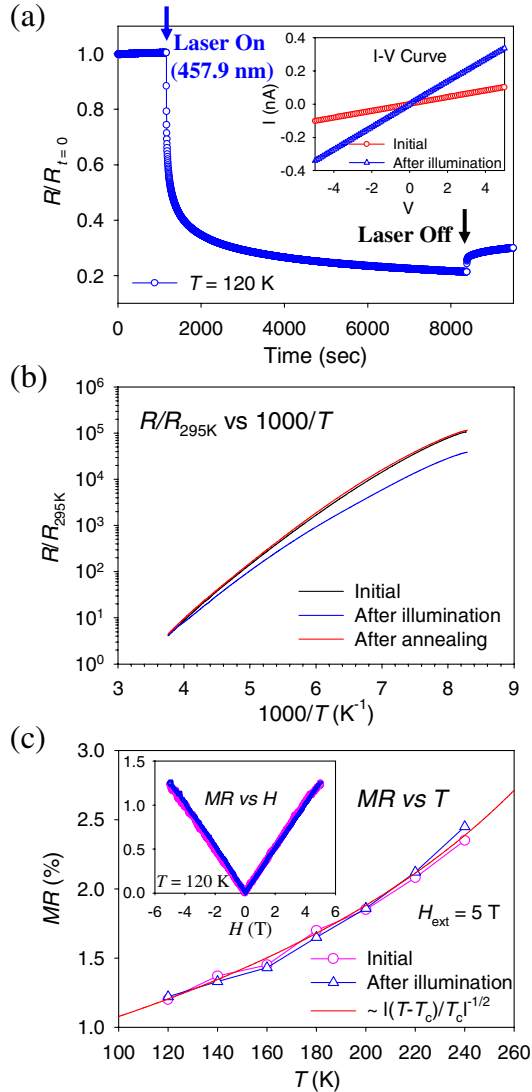
FIG. 2 (color online). (a) Normalized resistance of V(TCNE)$_x$ film upon illumination ($\lambda \sim 457.9$ nm, $I \sim 20$ mW/cm^2, at 120 K). Inset shows i-V curves before and after illumination at 120 K. (b) Normalized resistances as a function of temperature for both ground and photoexcited states [black: before illumination, blue: after illumination ($\lambda \sim 457.9$ nm, $I \sim 20$ mW/cm^2 for 2 h at 120 K), red: after warming sample to 280 K and waited for 10 min]. (c) Magnetoresistance (at 5 T) vs temperature for both ground and photoexcited states (illuminated at 120 K with $\lambda \sim 457.9$ nm, $I \sim 20$ mW/cm^2 for 2 h). Inset shows the typical linear behavior of MR vs H (0–5 T) at 120 K before/after illumination.

perature increases, and become identical above 250 K. The estimated effective energy gap at 130 K from the linear plot of $\log(R/R_{295\ K})$ versus $1000/T$ for the photoexcited state is 0.28 eV, which is 0.04 eV less than the value for the ground state.

V(TCNE)$_x$ exhibits an anomalous positive magnetoresistance MR $= [\rho(H, T) - \rho(0, T)]/\rho(0, T)$, which is explained by the role of magnetic energy in the activation energy gap [6,7]. In this model, the π^* band in (TCNE)$^-$ is

split into two subbands by the on-site Coulomb repulsion. Because of the antiferromagnetic interaction, the external magnetic field introduces a change of activation energy gap $\Delta E' = \Delta E - J\langle S\rangle\langle\sigma\rangle$ [6], where ΔE is the energy gap between conduction and valence bands, J is the magnetic exchange energy, $\langle S\rangle$ is the spin polarization of V^{2+}, and $\langle\sigma\rangle$ is the spin-1/2 polarization of the lower π^* subband. From mean field theory, far below T_c MR is $\sim h/|(T - T_c)/T_c|^{1/2}$, where $h = \mu_B H/k_B T_c$ [6]. Initially it was suggested that the thermal activation band gap is between the two spin-polarized π^* subbands of opposite spin [6]. However, recent resonant photoemission (RPE) analysis reports that the d levels of V^{2+} lie between the π^* and $\pi^* + U_c$ subbands and the estimated energy gap between the $3d$ states in V^{2+} and $\pi^* + U_c$ in (TCNE)$^-$ anion is 0.5 eV at room temperature [20]. Nevertheless, the antiferromagnetic exchange induced magnetic energy in the activation energy gap is expected to have the same role in anomalous MR behavior [6]. The temperature dependencies of MR of V(TCNE)$_x$ at 5 T for both the ground and photoexcited states are displayed in Fig. 2(c). The red line in Fig. 2(c) is the plot of $|(T - T_c)/T_c|^{-1/2}$. A quantitative fit yields $T_c \sim 410$ K. The MR of samples measured in the 0–5 T range has linear MR(H) behavior below T_c with an increase of 1.2% at $H = 5$ T and $T = 120$ K as shown in inset of Fig. 2(c). This is similar to the linear behavior of previously reported [6,7]. Although the resistance of V(TCNE)$_x$ decreases by a factor of 3 upon illumination, the normalized magnetoresistance (MR) is still linear and apparently overlaps with the same slope for both ground and photoexcited states [inset in Fig. 2(c)] indicating no change in the mechanism of MR associated with the Coulomb gap and spin-polarized valence and conduction bands.

The metastability of photoinduced effects for both magnetic and electronic properties of V(TCNE)$_x$ films suggests the presence of light-induced distortion in the overall structure. The mid-IR absorption spectrum in Fig. 3 shows
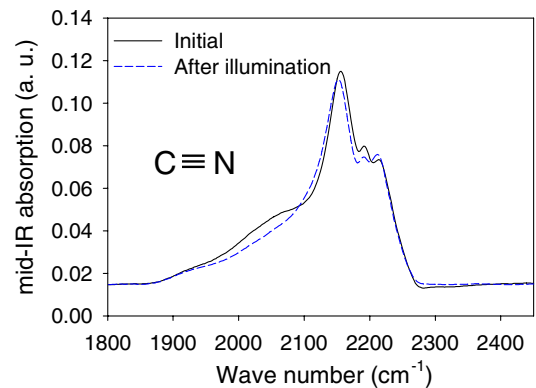
FIG. 3 (color online). Mid-IR spectra of CN stretching modes in V(TCNE)$_x$ film recorded at 10 K (black: initial spectrum, blue: recorded after 10 min of light illumination of $\lambda \sim 457.9$ nm and $I \sim 30$ mW/cm^2 at 10 K).

several features in the region 2050–2250 cm^{-1} [multiple peaks for CN vibrations are associated with different bridging, such as $trans$-μ-N, cis-μ-N, μ_4-(TCNE)$^-$, and possible modulation due to orbital overlap between N and V [5,15,24]]. Partial bleaching of CN vibration modes by the illumination ($\lambda \sim 457.9$ nm, $I \sim 30$ mW/cm^2, at 10 K for 10 min) supports the presence of photoinduced structural distortion. The $\pi \rightarrow \pi^* + U_c$ transition in (TCNE)$^-$ could introduce a structural change, since it can weaken the bonding within (TCNE)$^-$. Therefore, light excitation (2.7 eV) can introduce a transition from the ground state to an intermediate state, which can relax back to the original state and/or a metastable state with a local energy minimum, induced by structural relaxation.

The photoinduced magnetism is proposed to originate from photoinduced change in the orbital overlap of metal-to-ligand bonding, especially spin carrying orbitals [t_{2g} orbitals of V^{2+} and π^* orbitals of (TCNE)$^-$] and photo-induced structural changes. The change in the overlap integral of spin carrying orbitals induced by changes in (TCNE)$^-$ structures can explicitly modulate kinetic exchange interaction. We speculate the change in exchange energy could be spatially inhomogeneous due to the random structural change resulting in the increase of magnetic anisotropy and random magnetic order. Enhanced magnetic anisotropy in the photoexcited state may induce a decrease in magnetization below reentrant transition $T_r \sim$ 90 K and lead to a slight shift of T_r towards higher temperature. However, above this increased T_r no significant change is found in the overall magnetization, though the photoexcited metastable state can be fully erased only when warmed to 250 K.

On the other hand, the origin of the photoinduced conductivity is associated predominantly with the charge transfer integral between the orbitals of adjacent (TCNE)$^-$ in addition to the orbital overlap of the V^{2+} and (TCNE)$^-$ bond, which are related to carrier mobility and concentration. The photoinduced random structural change in the system could lead to broadening of π^* subbands so that the effective activation energy gap between the valence and conduction bands can be reduced producing a higher carrier concentration. The increased disorder could also create favorable directions at local sites for electron hopping resulting in stronger charge transport pathways. In short, the light-induced disorder in the system may result in both a higher carrier concentration, due to reduced activation energy gap, and increased mobility due to improved charge transfer overlap; however, stronger random magnetic order decreases overall magnetization at low magnetic fields.

In summary, we have reported multiple photonic effects in V(TCNE)$_x$ films through photoinduced magnetic, electronic, and spectroscopic studies. Both photoinduced mag-

netic and electrical properties originate from structural changes triggered by $\pi \rightarrow \pi^* + U_c$ excitation in (TCNE)$^-$. The photoexcited state, which exhibits reduced magnetic susceptibility and increased conductivity, is a long-lived metastable state at low temperature and can be fully recovered to the ground state by warming above 250 K. The organic-based hybrid magnet V(TCNE)$_x$ is a particularly interesting system not only for its room temperature magnetic order but also for its exotic spin-polarized electronic structure and transport properties. In addition, the demonstrated optical control of both magnetic and electrical properties may introduce a new paradigm in developing functional materials and devices associated with spintronics.

---

[1] S. A. Wolf *et al.*, Science **294**, 1488 (2001).
[2] H. Ohno, Science **281**, 951 (1998).
[3] T. Dietl *et al.*, Science **287**, 1019 (2000).
[4] J. M. Manriquez *et al.*, Science **252**, 1415 (1991).
[5] K. I. Pokhodnya, A. J. Epstein, and J. S. Miller, Adv. Mater. **12**, 410 (2000).
[6] V. N. Prigodin *et al.*, Adv. Mater. **14**, 1230 (2002).
[7] N. P. Raju *et al.*, J. Appl. Phys. **93**, 6799 (2003).
[8] O. Sato *et al.*, Science **272**, 704 (1996).
[9] D. A. Pejaković *et al.*, Phys. Rev. Lett. **85**, 1994 (2000).
[10] S. Ohkoshi *et al.*, J. Am. Chem. Soc. **128**, 5320 (2006).
[11] O. Kahn and C. J. Martinez, Science **279**, 44 (1998).
[12] P. Gütlich and H. A. Goodwin, Top. Curr. Chem. **233**, 1 (2004).
[13] S. Koshihara *et al.*, Phys. Rev. Lett. **78**, 4617 (1997).
[14] K. Matsuda *et al.*, Phys. Rev. B **58**, R4203 (1998).
[15] D. A. Pejaković *et al.*, Phys. Rev. Lett. **88**, 057202 (2002).
[16] J. Zhang *et al.*, Angew. Chem., Int. Ed. Engl. **37**, 657 (1998).
[17] A. Zheludev *et al.*, Angew. Chem., Int. Ed. Engl. **33**, 1397 (1994).
[18] D. Haskel *et al.*, Phys. Rev. B **70**, 054422 (2004).
[19] C. Tengstedt *et al.*, Phys. Rev. B **69**, 165208 (2004).
[20] C. Tengstedt *et al.*, Phys. Rev. Lett. **96**, 057209 (2006).
[21] See EPAPS Document No. E-PRLTAO-97-079649 for SEM image of CVD-deposited V(TCNE)$_x$ film. For more information on EPAPS, see http://www.aip.org/pubservs/epaps.html.
[22] See EPAPS Document No. E-PRLTAO-97-079649 for comparison of 2-probe and 4-probe resistance measurements. For more information on EPAPS, see http://www.aip.org/pubservs/epaps.html.
[23] G. Du *et al.*, J. Appl. Phys. **73**, 6566 (1993).
[24] J. S. Miller, Angew. Chem., Int. Ed. **45**, 2508 (2006).